Synthesis, Molecular Structure, Spectral Investigation on (E)-3-(3-4-Dibromophenyl)-1-(2-Methoxyphenyl) Prop-2-En-1-One

S.Syed Shafi[1] P.Chakkaravarthy[2]
[1, 2] Dept of Chemistry
[1]Thiruvalluvar University, Vellore, Tamil nadu India
[2] Government Thirumagal Mills College Gudiyattam, India

Abstract- *The title compound, The chemical name is (E)-3-(3-4-dibromophenyl)-1-(2-methoxyphenyl)prop-2-en-1-one (EDMPP) was synthesized and characterized by FT-IR and FT-Raman spectral analysis. The optimized molecular geometry, the vibrational wavenumbers, the infrared intensitie and the Raman scattering activities were calculated by using density functional theory(DFT) B3LYP method with 6-311++G(d,p) basis set. The detailed interpretation of the vibrational spectra has been carried out by VEDA program. Stability of the molecule arising from hyperconjugative interactions, charge delocalization have been analyzed using natural bond orbital analysis (NBO). The first order hyperpolarizability was also performed.*

Keywords- FT-IR, FT-Raman, NLO, NBO, antimicrobial, molecular docking FT-IR, FT-Raman, NLO, NBO, antimicrobial, molecular docking Corresponding Author: P.chakkaravarthy,M.Sc,M.Phil.

I. INTRODUCTION

Chalcones belong to flavonoid family. The chemical name is (E)-3-(3-4-dibromophenyl)-1-(2-methoxyphenyl)prop-2-en-1-one (EDMPP); they consist of open-chain flavonoids in which the two aromatic rings are joined by a three-carbon, α-unsaturated carbonyl system. A vast number of naturally occurring chalcones are polyhydroxylated in the aryl rings. The radical quenching properties of the phenolic groups present in many chalcones have raised interest in using the compounds or chalcone rich plant extracts as drugs or food preservatives. Chalcones have been reported to possess many useful properties, including anti-inflammatory, antimicrobial, antifungal, antioxidant, cytotoxic, anticancer activities. Many chalcones have been described for their high antimalarial activity. Chalcones a derivative with 4-bromophenyl and 2-methoxy rings bonded at the opposite ends of a propenone group, the biologically active region [1-5].

A through literature analysis made over a decade reveals the need for analyzing the title compound theoretically to support experimental observations. Hence an attempt has been made in present work to analyze this titled compound theoretically and supports these results experimentally. To our knowledge and literature survey reveals that there are no theoretical calculations or detailed vibrational analysis have been performed on 2(E) molecule so far. A systematic study of the molecule structure and vibrational spectra help in understanding the property of title molecule in-depth insight.Vibrational spectra of the title compounds have been analyzed on the basis of potential energy distribution (PED). The change in electron density(ED) in the σ* and π* antibonding orbitals and stabilization energies E(2) have been calculated by natural bond orbital (NBO)analysis to give clear evidence of stabilization originating in the hyperconjugation of hydrogen-bonded interaction. By analyzing the total (TDOS) and αβ DOS density of states, the molecular orbital composition and their contributions to the chemical bonding were studied.

1.2 Material and method

1.2.1Experimental details

The compound EDMPP was prepared by following the procedure reported by Sreevidya*et al.*[6] for the preparation of chalcones. The chalcone formed was purified by recrystallization from absolute alcohol(M.P.453-455K). The FT-IR spectrum of the sample was recorded in the region 4000-400 cm^{-1} in evacuation mode using KBr pellet technique with 1.0 cm resolution on a PERKINELMER FT-IR spectrophotometer. The FT-Raman spectrum of the sample was recorded in the region 4000-100 cm^{-1} in a pure mode using Nd; YAG laser of 100 with 2 cm resolution on BRUKER RFS 27 at SAIF, IIT, Chennai, India.

1.2.2Computational details

The optimized structure of the title compound, corresponding energy, and vibrational harmonic frequencies was calculated by using DFT (B3LYP) / 6-311++G(d, P) basis set using GAUSSIAN 03W program package [7]. Without any constraint on the geometry the energy of the title molecule was minimized, whole intramolecular forces were brought to be zero. The geometry was optimized at B3LYP level by using 6-311++G(d,p) basis set. The frequency calculation delivered the fundamental vibrational frequencies, optimized geometrical parameters, energy, thermodynamical data such as entropy, enthalpy, and heat capacity. Also, IR and Raman spectra were stimulated. Mulliken population analysis determined the distribution of electrons into the molecular orbitals. The symmetries of the vibrational modes were determined by using the standard procedure [8] of decomposing the traces of the symmetry operation into the irreducible representations. By combining the result of the Gaussview program [9] with symmetry considerations, vibrational frequency assignments were performed. Calculation of potential energy distribution (PED) and the prediction of IR and Raman intensities were done with VEDA 4 program [10]. The NBO analysis and MEP calculations were performed on the title molecule. NBO give clear evidence stabilization originating from hyperconjugation of various intramolecular interactions [11-13]. The Mulliken populations were reported. The molecular orbital compositions and their contributions to the chemical bonding are studied by Total density states (TDOS) and the sum of α and β electron density of states (αβTDOS). Furthermore, various non-linear optical properties of EDMPP such as dipole moment, the anisotropy of polarizability and first-order hyper polarizability were also computed on theoretical computations.

1.2.3Prediction of Raman intensities

The Raman activities (S_i) calculated by Gaussian 03 program have been suitably adjusted by the scaling procedure with MOLVIB and subsequently converted to relative Raman intensities *(I_i)* using the following relationship derived from the basic theory of Raman scattering [14].

$$I_i = \frac{f(\upsilon_0-\upsilon_i)^4 S_i}{\upsilon_i [1 - \exp (hc\upsilon i/k_b T)]} ,$$

Where v_o is the exciting frequency (in cm), $v_i$is the vibrational wave number of the *ith* normal mode, h,c, and k are universal constants, and the f is the suitably chosen common scaling factor for all the peak intensities. For the plots of simulated IR and Raman spectra, pure Lorentzian band shapes are used with a full width at half maximum of 10 cm^{-1} [15].

1.3 Results and Discussion

1.3.1 Geometrical structure

The optimized structure parameters of EDMPP was calculated at B3LYP levels with the 6-311++G(d,p) basis set and are listed in Table 1. in accordance with the atom numbering scheme as obtained from CHEMCRAFT software Fig 1.The table 1 of comparison for the experimental XRD data available from the literature [16] and the calculated bond angle and bond length for EDMPP is given in Table1.While comparing these values we can see that both are nearly the same, in case of any slight deviation is due to the fact that the theoretical calculations belong to the molecule in the gaseous phase and the experimental results belong to the solid phase [17,18]. In spite of the slight difference in the calculated geometrical parameters, they represent a good approximation and they form the base for calculating other parameters such as vibration frequencies and thermodynamic properties [19-21].This molecule has sixteen C – C bond lengths, two C – O bond length, twelve C – H bond lengths and two C – Br bond length. It is observed that the calculated C – C bond distances are higher than the C – N bond lengths, they are found to the be slight difference at all levels of calculations. From theoretical values, we found most of the optimized bond lengths are in good agreement with experimental bonds lengths, but bond angles are slightly longer and shorter than that of experimental values.

1.3.2Vibrational Assignments

The experimental FT-IR and FT-Raman spectra for (E)-3-(3-4-dibromophenyl)-1-(2-methoxyphenyl)prop-2-en-1-one (EDMPP)are shown in Fig 2 and Fig 3. The vibrational frequencies calculated at B3LYP/6-311++G(d,p) levels were scaled to a factor 0.9641. The vibrational frequencies along with the approximate description of each normal mode of vibration obtained using the basis set B3LYP/6-311++G(d,p) are given in Table 2. The relative intensities were obtained by dividing the computed value by the intensity of the strongest line. Computed intensities and the observed values show intermediate deviation since the computed wave numbers correspond to the isolated molecular state whereas the observed wave numbers corresponding to the solid state spectra. ChemCraft, which is a graphical interface, was used to assign the calculated harmonic wave numbers using displacement vectors to identify the motion of modes.The predicted vibrational wave numbers and the experimental data are well in agreement with each other.

1.3.2.1 C-H Vibrations

The hetero aromatic structure shows the presence of C-H stretching vibrations in the region 3100-3000 cm^{-1}[22] which is the characteristic region for the ready identification of C-H vibration. In these compounds C-H vibration absorption bands are usually weak; in many cases, it is too weak for detection. Scaled vibrations assigned to the aromatic C-H stretching computed in the range 3174, 3101, 3090, 3089, 3086, 3075, 3073, 3057, 3050, 3042, 3026, 2959, 2899 cm^{-1} by B3LYP/6-311++G(d,p) method shows good agreement to the experimental FT-IR at 3060, 2983 cm^{-1} and FT-Raman at 3062 and 3018 cm^{-1}.

1.3.2.2 C-C Vibrations

The C-C aromatic stretching vibrations give rise to characteristic bands in both the observed IR and Raman spectra covering the spectral range from 1500 – 1650cm^{-1}[23,24]. In general, the bands are of variable intensity and according to Varsanyi, the five bands in this region are observed at 1489,1433, 1371,1332,1283,1228,1162. Neville and Shrvell have identified the IR bands at 1470, 1484, 1561, 1575, 1590cm^{-1} in diazepam and closely related compounds of benzodiazepines due to aromatic C-C stretching vibrations. Based on these factors, in the present study, the stronger C-C vibrations occurs at 1590, 1600cm^{-1} in the FT-IR spectrum and 1577, 1596cm^{-1} in the FT-Raman spectrum.

1.3.2.3 C = O Vibrations

The carbonyl stretching frequency has been most extensively studied by infrared spectroscopy [25]. This multiple bonded group is high polar and therefore give rise to an intense infrared absorption band. In the present study, the carbonyl stretching vibrations are found in the region of 1780 – 1700 cm [26]. In our present study, the strong band at 1775 cm^{-1} in FT-IR and1737 cm^{-1} as a weak band in FT-Raman spectrum are assigned to C–O stretching vibration shows small deviation calculated byB3LYP/6-311++G(d,p) method at 1678 cm^{-1} with PED contribution of 90%, the shift of the C-O stretching frequency to the low-frequency side indicate the presence of a strong intermolecular hydrogen bonding, as discussed above in this manuscript.The C-O out of plane bending is observed as intense bands in the IR spectrum in the expected regions [27] at 782 cm^{-1} in FT-IR spectrum.

1.3.2.4 C – Br Vibrations

The vibrations belonging to the bond between the ring and the halogen atoms are worth to discuss here since mixing of vibrations is possible due to the lowering of the molecular symmetry and the presence of heavy atoms on the periphery of the molecule. Generally, the C – Br absorption is obtained in the region between850 and 550 cm^{-1} [28]. Therefore, the strong band found at669 cm^{-1} in the FT-IR spectrum has been designated to C – Br stretching mode of vibration and at 687 cm^{-1} in the FT-Raman spectrum with 70% PED contribution. The band identified at 310 cm^{-1} in Raman is assigned to the C – Br out of torsion-plane mode.

1.4 NLO properties

Non-linear optical (NLO) effects arise from the interactions of electromagnetic fields in various media to produce new fields altered in phase, frequency, amplitude or other propagation characteristics from the incident fields. NLO is at the forefront of current research because of its importance in providing the key functions of frequency shifting, optical modulation, optical switching, optical logic and optical memory for the emerging technologies in areas such as telecommunications, signal processing and optical interconnections [29-31]. Organic molecules that exhibit extended p conjugation, in particular, show enhanced second-order NLO properties. [32,33].

The first hyperpolarizability(β) of this novel molecular system and the related properties (μ, α, β_0) of LAO are calculated using the B3LYP/6-311++G(d,p) basis set, based on the finite field approach. In the presence of an applied electric field, the energy of a system is a function of the electric field. The first hyperpolarizability is a third-rank tensor that can be described by a 3 x 3 x 3 matrix. The 27 components of the 3D matrix can be reduced to 10 components due to the Klein man symmetry [34]. It can be given in the lower tetrahedral. The components are defined as the coefficients in the Taylor series expansion of the energy in the external electric field. When the external electric field is weak and homogenous, this expansion becomes:

$$E = E^{O} - \mu\alpha F\alpha - 1/2\alpha\alpha\beta F\alpha F\beta - 1/6\beta\alpha\beta\gamma F\alpha F\beta F\gamma + \ldots..$$

The total static dipole moment is

$$\mu = (\mu^2_x + \mu^2_y + \mu^2_z)^{1/2}$$

The isotropic polarizability is

$$\alpha_0 = \alpha_{xx} + \alpha_{yy} + \alpha_{zz}/3$$

The polarizability anisotropy invariant is

$$\alpha = 2^{1/2}[(\alpha_{xx} - \alpha_{yy})^2 + (\alpha_{yy} - \alpha_{zz})^2 + (\alpha_{zz} - \alpha_{xx})^2 + 6\,\alpha^2_{xx}]^{1/2}$$

and the average hyperpolarizability is

$$\beta = (\beta^2_x + \beta^2_y + \beta^2_z)^{1/2}$$

$$\beta_x = \beta_{xxx} + \beta_{xyy} + \beta_{xzz}$$

$$\beta_y = \beta_{yyy} + \beta_{xxy} + \beta_{yzz}$$

$\beta_z = \beta_{zzz} + \beta_{xxy} + \beta_{yyz}$

Where E^o is the energy of the unperturbed molecules, F is the field at the origin and are the components of dipole moment, polarizability, and first-order hyperpolarizabilities, respectively. The total static dipole moment (μ), polarizability (α) and the first order hyperpolarizability(β), using the x,y,z components are defined as follows. The calculated hyperpolarizability values of EDMPP are listed in Table 3. According to the present calculation values of dipole moment and first-order hyperpolarizability of (E)-3-(3-4-dibromophenyl)-1-(2-methoxyphenyl)prop-2-en-1-one (EDMPP) from B3LYP/6-311++G(d,p) basis set are 1.4348 Debye and 1.5741 esu as shown in Table 3. The total dipole moment of the title molecule is approximately only one time greater than those of the urea (1.3732 D) and the first hyperpolarizability of the molecule is approximately four times greater than those of urea (0.372 esu).Based on these facts, it could be concluded that the present material has a reasonably good propensity for nonlinear optical activity.

1.5 NBO analysis

NBO analysis transforms molecular orbital wave functions into one-center (lone pair) and two-center (bond) representations [35]. The advantage of NBO analysis is that they provide insight into the interactions between various parts of the molecule [36]. The bond-anti bond and lone-pair-anti bond interactions can be calculated by two difference procedures following the NBO method [37]. The first one is an indirect procedure as suggested by Weinhold, which involves comparison of barrier energies calculated with and without the Fock matrix element (F_{ij}) [38]. The second procedure involves the estimations of all possible interactions between “filled” (donor) Lewis type NBO s and “empty” (acceptor) non-Lewis NBOs, by considering their energetic importance using second-order perturbation theory. Since these interactions lead to the donation of occupancy from the localized NBOs of the idealized Lewis structure into the empty non-Lewis orbitals, they are referred to as “delocalization” corrections to the zeroth-order natural Lewis structure. For each donor, NBO (i) and acceptor (j), the stabilization energy E(2) associated with delocalization i –> j is represented as:

$$E(2) = \Delta E_{ij} = q_i (F_{ij})^2 / (\varepsilon_j - \varepsilon_i)$$

Where q_i is the donor orbital occupancy, F_{ij} is the off-diagonal and $\varepsilon_j, \varepsilon_i$ are diagonal elements specifying the respective orbital energies of the NBO Fock matrix.

NBO analysis has been performed on the molecule at the B3LYP/6-311+ +G (d,p) level in order to elucidate the intra molecular, rehybridization and de-localization of electron density within the molecule. The strong intramolecular hyper conjugative interaction of the σ and π electrons of C-C to the antibonding C – C bond in the ring leads to stabilization of some part of the ring as evident from Table 4. The intramolecular hyperconjugative interactions of the σ and π electrons of C-H to the antibonding C -H bond in the ring leads to stabilization of some part of the ring as evident from the Table4. The intramolecular hyperconjugative interactions of σ (C_{10} - H_{25}) orbital to σ*(C_3 - H_{21}) and σ (C_3 - H_{21}) orbital to σ*(C_{10}- H_{25}) leads to strongest stabilization energy of 206 k J/mol and 200 k J/mol. For π(C_2 - C_3) orbital to π*(C_1 - O_4) shows the stabilization energy of 29.35 k J/mol. Similarly, π(C_5 - C_6) bonding orbital to antibonding orbital π* (C_1 - O_4) and (C_9 - C_{10}) shows the highest energy of 27.78 k J/mol and 24.37 k J/mol. Therefore, the maximum energy delocalization takes place in the π to π* transition. The E(2) values and types of the transition are shown in Table 4.

Molecular docking

Molecular docking is a key tool in structural molecular biology and computer-assisted drug design. Auto Dock is a collection of automated docking tools arrange to predict how miniature scale molecules, such as substrates or drug candidate, bind to a receptor of known three dimensional structures. The aim to investigate the binding mode, a molecular modeling study was performed and EDMPP was selected to be docked into the active site oftwo receptors ZH4Z, and 4Y95 [39] of antimicrobial proteins which was downloaded from RCSB protein data bank [40]. Docked conformation which had the lowest binding energy was chosen to investigate the mode of binding. The molecular docking binding energies (kcal/mol) and inhibition constants (μm) were also obtained and listed in Tabl.5. Among them, 4Y95 exhibited the lowest free energy at -7.03 kcal/mol and most docked inhibitors interacted with the ligand within the 4Y95 binding site. They exhibited up to three hydrogen bonds involving TRP 395,ILE 347and TRP 421 with RMSD being 36.958 Å. The docking simulation shows the best binding mode of the EDMPP into 4Y95 The EDMPP ligand interacts with different receptors are shown in Figs.4,5.

1.11 Conclusion

In the present work, we have thoroughly analyzed spectroscopic (FT-IR, FT-Raman), NLO and NBO analysis of EDMPP molecule with B3LYP/6-311++G(d,p)methods.The

structural parameters, vibrational frequencies, infrared intensities and Raman activities calculated by B3LYP/6-311++G(d,p)methods 311++G(d,p) method agree very well with experimental results. The complete vibrational assignments of wave numbers are made on the basis of potential energy distribution (PED). The nonlinear optical properties are also addressed theoretically. The first order hyperpolarizability of the title compound is twenty six times greater than the value of urea. Furthermore, antimicrobial studies of the title molecule show that a molecule is an attractive object for the future studies of biological activity.

REFERENCES

[1] S. Y. Kim, I. S. Lee and A. Moon, Chem.-Biol. Interact., 203 (2013) 565.

[2] J. Zhang, Ch. Sun, Y. Yan, Q. Chen, F. Luo, X. Zhu, X. Li and K. Chen, Food Chem., 135 (2012) 1471.

[3] V. R. Yadav, S. Prasad, B. Sung and B. B. Aggarwal, Int. Immunopharmacol., 11 (2011) 295

[4] A. Modzelewska, C. Pettit, G. Achanta, N. E. Davidson, P. Huang and S. R. Khan, Bioorg. Med. Chem., 14 (2006) 3491.

[5] M. V. Reddy, C. R. Su, W. F. Chiou, Y. N. Liu, R. Y. Chen, K. F. Bastow, K. H. Lee and T. S. Wu, Bioorg. Med. Chem., 16 (2008) 7358.
T.V. Sreevidya, B. Narayana, H.S.Yathirajan,Central European Journal of Chemistry 8 (2010)174-181

[6] Gaussion 03 Program, Gaussian Inc., Wallingford, CT, 2004.

[7] P. Hohenberg, W. Kohn, Phys. Rev. 136 (1964) B864–B871.

[8] A. Frisch, A.B. Neilson, A.J. Holder, Gauss View Users Manual, Gaussian Inc.,Pittsburgh, PA, 2000.

[9] M.H. Jamroz, Vibrational Energy Distribution Analysis: VEDA 4 Program, Warasaw, Poland, 2004.

[10] X.-H. Li, R.-Z. Zhang, X.-Z. Zhang, Struct. Chem. 20 (2009) 1049–1054.

[11] J. Chocholousova, V. VladiminSpirko, P. Hobza, Phys. Chem. 6 (2004) 37–41.

[12] A.E. Reed, L.A. Curtiss, F. Weinhold, Chem. Rev. 88 (1988) 899–926.

[13] G. Keresztury, S. Holly, J. Varga,, G. Besenyei, A.Y. Yang, J.R. Durig, SpectrochimActa A 49 (1993), pp: 2007-2026.

[14] G. Keresztury, in: J.M. Chalmers, P.R. Griffth (Eds.), Raman Spectroscopy: Theory in Handbook of vibrational spectroscopy, vol 1, John Wiley & Sons Ltd., New York, 2002

[15] N. Subramanian, N. Sundaraganesan, J. Jayabharathi, Spectrochim. Acta A 76 (2010) 259–269.

[16] H.B. Schlegel, J. Comput. Chem. 3 (1982) 214–218.

[17] Socrates, Infrared and Raman Characteristics Group Frequencies, Tables and Charts, third ed., Wiley, Chichester, 2001.

[18] R. Shanmugam, D. Sathyanarayanan, Spectrochim. Acta A 40 (1984) 757–761.

[19] P. Vandenabeela, L. Moens, H.G.M. Edwards, R. Dams, J. Raman Spectrosc. (2000) 509–566.

[20] P.J. Trotter, Appl. Spectrosc. 31 (1977) 30–38.

[21] D.N. Sathyanarayana, Vibrational Spectroscopy – Theory and Applications,second ed., New Age International (P) Limited Publishers, New Delhi, 2004.

[22] Y.X. Sun, Q.L. Hao, Z.X. Yu, W.X. Wei, L.D. Lu, X. Wang, Mol. Phys. 107 (2009) 23–235.

[23] J.P. Abraham, D. Sajan, V. Shettigar, S.M. Dharmaprakash, Nemec, I.H. Joe, V.S.

[24] K.B. Wiberg, A. Shrake, Spectrochim. Acta A 29 (1973) 583–587.

[25] G. Varsanyi, Vibrational Spectra of Benzene Derivates, Academic Press, New York, 1969.

[26] M. Szafran, A. Komasa, E.B. Adamska, J. Mol. Struct. THEOCHEM 827 (2007) 101–110.

[27] M. Arivazhagan, S. Jeyavijayan, Spectrochim. Acta A 79 (2011) 376–383

[28] M. Nakano, H. Fujita, M. Takahata, K. Yamaguchi, J. Am. Chem. Soc. 124 (2002) 9648–9655.

[29] V.M. Geskin, C. Lambert, J.L. Bredas, J. Am. Chem. Soc. 125 (2003) 15651–15658.

[30] D. Sajan, H. Joe, V.S. Jayakumar, J. Zaleski, J. Mol. Struct. 785 (2006) 43–53.

[31] J. Indira, P.P. Karat, B.K.Sarojini , J. Crystal Growth 242 (2002) 209-214

[32] B.K. Sarojini, B. Narayana, B.V. Ashalatha, J. Indira, K.G. Lobo, J. Crystal Growth 295 (2006) 54–59

[33] S.T. Kanchana, K.M. Nalin de Silva, J. Mol. Struct. (Theochem) 617 (2002) 169–175.

[34] J. Karpagam, N. Sundaraganesan, S. Sebastian, S. Manoharan, M. Kurt, J. Raman Spectrosc. 41 (2010) 53–62.

[35] A.E. Reed, F.J. Weinhold, Chem. Phys. 78 (1993) 4066–4073.

[36] L. Goodman, H. Gu, J. Chem. Phys. 109 (1998) 72–78.

[37] A.E. Reed, F. Wienhold, Isr. J. Chem. 31 (1991) 277–285.

[38] Ravi Kumar A, Sathaiah G, Chandra Shekhar A, Raju K, Shanthan Rao P, Narsaiah B et al. Synthesis of 6-Fluoro-7-cyclic Amino-substituted Dicarboxylic Acid Quinolones and their Antibacterial Activity, J. Hetercycl Chem, 2014; 51:114-122.

[39] Joselin Beaula T, Hubert Joe I, Rastogi VK, Bena Jothy V, Spectral investigations. DFT computations and

molecular dockingstudies of the antimicrobial 5-nitroisatin dimer, Che. Phy. Letters, 2015; 624:93-101.

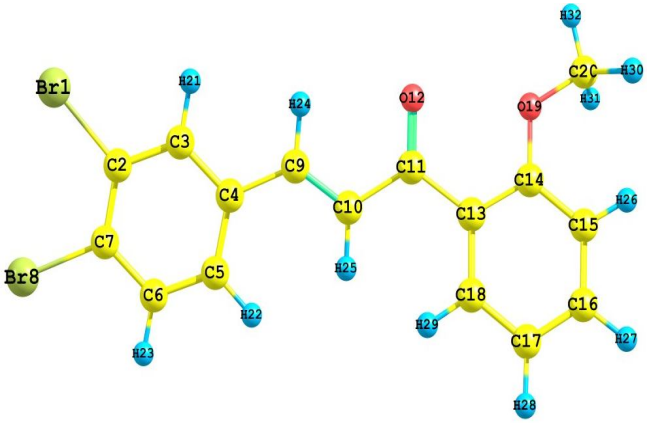

Fig 1. Optimized structure of EDMPP

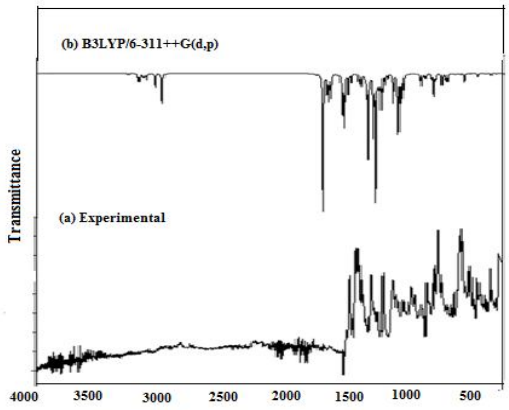

Wavenumber cm-1

Fig.2. (a) Experimental (b) theoretical FT-IR spectra of EDMPP

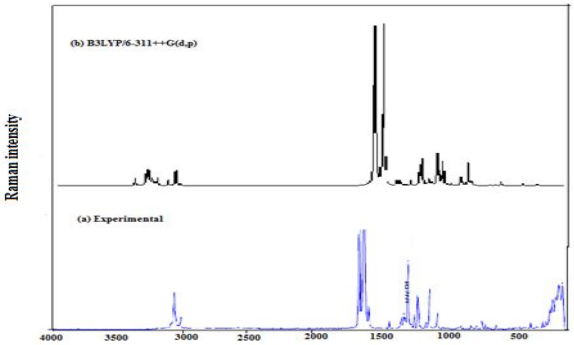

Wavenumber cm-1

Fig.3. (a) Experimental (b) theoretical FT-Raman spectra of EDMPP

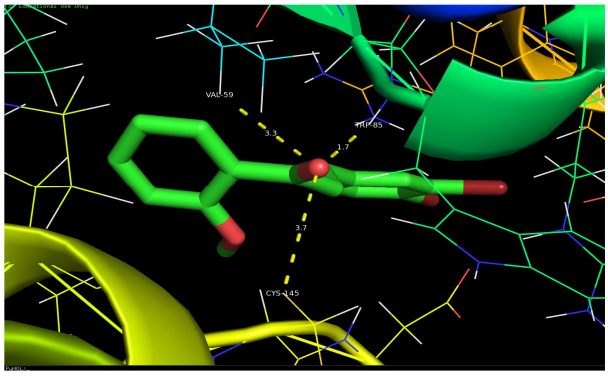

Fig 4: Docking and Hydrogen bond interactions EDMPP with chain A of ZH4Z protein structure

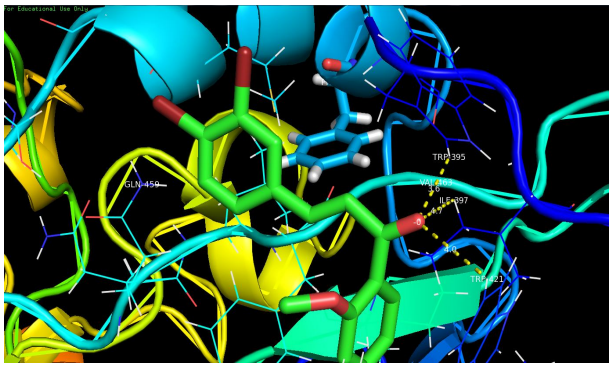

Fig 5: Docking and Hydrogen bond interactions EDMPP with chain A of 4Y95 protein structure

Table 1. Optimized geometrical parameters bond length and bond angles of title molecule by B3LYP/6-311++G(d,p) in comparison with experimental values

Parameter table	Experimental	B3LYP/6-311++G(d,p)	Parameter table	Experimental	B3LYP/6-311++G(d,p)
Bond length					
C_1 - C_2	1.517	1.505	C_2 - C_3 - H_{21}	120	121
C_1 - O_4	1.208	1.224	C_{13} - C_3 - H_{21}	120	119
C_1 - C_5	1.517	1.503	C_3 - C_{13} - C_{14}	120	119
C_2 - C_3	1.337	1.345	C_3 - C_{13} - C_{18}	120	120
C_2 - H_{20}	1.1	1.086	C_6 - C_5 - C_{10}	120	120
C_3 - C_{13}	1.503	1.47	C_5 - C_6 - C_7	120	120
C_3 - H_{21}	1.1	1.081	C_5 - C_6 - O_{11}	120	120
C_5 - C_6	1.42	1.43	C_5 - C_{10} - C_9	120	120
C_5 - C_{10}	1.42	1.402	C_5 - C_{10} - H_{25}	120	120
C_6 - C_7	1.42	1.403	C_7 - C_6 - O_{11}	120	121
C_6 - O_{11}	1.355	1.347	C_6 - C_7 - C_8	120	121
C_7 - C_8	1.42	1.389	C_6 - C_7 - H_{22}	120	120
C_7 - H_{22}	1.1	1.08	C_6 - O_{11} - C_{12}	120	120
C_8 - C_9	1.42	1.39	C_8 - C_7 - H_{22}	120	119
C_8 - H_{23}	1.1	1.084	C_7 - C_8 - C_9	120	120
C_9 - C_{10}	1.42	1.389	C_7 - C_8 - H_{23}	120	119
C_9 - H_{24}	1.1	1.083	C_9 - C_8 - H_{23}	120	120
C_{10} - H_{25}	1.1	1.075	C_8 - C_9 - C_{10}	120	119
O_{11} - C_{12}	1.4	1.422	C_8 - C_9 - H_{24}	120	120
C_{12} - H_{26}	1.11	1.088	C_{10} - C_9 - H_{24}	120	120
C_{12} - H_{27}	1.11	1.095	C_9 - C_{10} - H_{25}	120	120
C_{12} - H_{28}	1.11	1.095	O_{11} - C_{12} - H_{26}	109	109
C_{13} - C_{14}	1.42	1.404	O_{11} - C_{12} - H_{27}	109	110
C_{13} - C_{18}	1.42	1.406	O_{11} - C_{12} - H_{28}	109	110
C_{14} - C_{15}	1.42	1.392	H_{26} - C_{12} - H_{27}	109	109
C_{14} - H_{29}	1.1	1.085	H_{26} - C_{12} - H_{28}	109	109
C_{15} - C_{16}	1.42	1.39	H_{27} - C_{12} - H_{28}	109	109
C_{15}- Br_{30}	1.88	1.082	C_{14} - C_{13} - C_{18}	120	119
C_{16} - C_{17}	1.42	1.394	C_{13} - C_{14} - C_{15}	120	120

C_{16} - Br_{19}	1.88	1.915	C_{13} - C_{14} - H_{29}	120	120
C_{17} - C_{18}	1.42	1.388	C_{13} - C_{18} - C_{17}	120	120
C_{17} - H_{31}	1.1	1.082	C_{13} - C_{18} -H_{32}	120	120
C_{18} - H_{32}	1.1	1.083	C_{15}- C_{14} -H_{29}	120	120
Bond angles			C_{14} - C_{15} - C_{16}	120	120
C_2 - C_1 - O_4	120	119	C_{14} - C_{15} - H_{30}	120	120
C_2 - C_1 - C_5	120	119	C_{16} - C_{15} - H_{30}	120	120
C_1 - C_2 - C_3	120	120	C_{15} - C_{16} - C_{17}	120	120
C_1 - C_2 - C_{20}	120	120	C_{15} - C_{16} - Br_{19}	120	120
O_4 - C_1 - C_5	120	120	C_{17} - C_{16} - Br_{19}	120	120
C_1 - C_5 - C_6	120	120	C_{16} - C_{17} - C_{18}	120	120
C_1 - C_5 - C_{10}	120	121	C_{16} - C_{17} - H_{31}	120	120
C_3 - C_2 - H_{20}	120	118	C_{18} - C_{17} - H_{31}	120	120
C_2 - C_3 - C_{13}	120	120	C_{17} - C_{18} - H_{32}	120	120

[a]Taken from Ref.[16]

Table 2.Vibrational wave numbers obtained for at DFT/6-311++G(d,p) [(harmonic frequency cm-1, IR intensities (K mmol-1, Raman intensities (units)].

S.No	Observed frequencies(cm-1)		Calculated frequencies(cm-1) DFT/6-311++G(d,p)				Vibrational modes (>10% PED)
	FT-IR	FT-Raman	unscaled	scaled[a]	IR[b]	Raman[c]	
90	3305(w)	3300(w)	3292	3174	4	111	v CH (94)
89	3234(w)	-	3217	3101	8	154	v CH (95)
88	-	3210(w)	3205	3090	15	30	v CH(90)
87	-	3204(w)	3204	3089	2	140	v CH (93)
86	3201(w)	3200(w)	3201	3086	3	81	v CH (89)
85	-	-	3189	3075	18	176	v CH (96)
84	3198(vw)	3190(w)	3188	3073	1	20	v CH(97)
83	-	3176(w)	3170	3057	3	85	v CH (97)
82	3100(vw)	3160(w)	3164	3050	6	48	v CH (95)
81	-	-	3156	3042	8	46	v CH (96)
80	-	3018(w)	3139	3026	16	110	v CH (92)
79	3060(w)	3062(m)	3069	2959	34	86	v CH (100)
78	3005(w)	3018(w)	3007	2899	75	224	v CH (92)

77	-	-	1678	1618	304	866	v OC (79)
76	-	-	1675	1615	59	1783	v CC(57) +β HCCC(14)
75	-	1639(s)	1639	1580	45	89	v CC(66)
74	1633(ms)	1620(vs)	1623	1565	63	2352	v CC(31)
73	1572(ms)	1589(s)	1604	1547	55	305	v CC(37)
72	1566(s)	1563(ms)	1597	1539	12	97	v CC(45) + β CCC(10)
71	-	-	1519	1464	42	22	β HCC(94)
70	-	-	1514	1459	78	65	β HCH (67)
69	-	-	1498	1444	120	22	β HCC(25) + β HCH(29)
68	-	-	1497	1443	9	15	β HCH (67)+tHCOC(17)
67	1484(s)	-	1489	1435	1	35	v CC (10)+β HCC(29) + β HCH (21)
66	-	1404(vw)	1463	1410	50	18	β HCC(42) + β HCH (45)
65	1418(s)	-	1433	1381	22	77	v CC (32) + β HCC(22)
64	-	-	1371	1322	17	159	v CC(12) + β HCC(43)
63	1351(s)	-	1358	1309	29	385	β HCC(64)
62	-	-	1332	1285	3	7	v CC(66)
61	-	-	1327	1279	8	26	β HCC(76)
60	-	1306(w)	1313	1266	48	96	v CC(23) + v OC(13) + β HCC(10)
59	-	1286(w)	1298	1251	205	74	v OC(23)
58	1268(s)	1272(w)	1283	1237	20	37	v CC(12)
57	-	1253(ms)	1251	1206	150	473	v CC(43)
56	-	-	1228	1184	311	137	v CC(18) + β HCC(10)
55	-	1206(w)	1209	1165	13	347	β HCC(72)
54	-	-	1202	1159	24	14	β HCC(13) + t HCOC(56)
53	-	1176(ms)	1189	1146	84	3	β HCC (72)
52	1168(ms)	-	1164	1122	1	2	β HCC(28) + t HCOC(72)
51	-	-	1162	1120	24	31	v CC(30) + β HCC(18)
50	1134(ms)	1123(w)	1135	1094	12	2	v CC(27) + β HCC(55)
49	1068(ms)	1087(ms)	1086	1047	28	108	v CC(27) + v BrC(10)
48	-	-	1085	1046	47	17	v CC (29)
47	-	-	1049	1011	47	4	v OC(65) + β CCC(13)
46	-	1032(w)	1042	1004	136	339	v CC(18) + β CCC(28)
45	-	-	1022	985	66	60	β CCC(85)

44	1001(ms)	-	1007	971	34	0	t HCCC(87)
43	983(ms)	-	980	945	1	0	t HCCC(72) + t CCCC(12)
42	-	964	978	943	1	0	t HCCC(73) + t CCCC(11)
41	-	-	959	924	1	2	t HCCC(68) + t CCCC(10)
40	945(w)	-	930	896	0	1	t HCCC(74)
39	-	-	893	861	1	10	t CCCC(29) + out of tor OCCC(14)
38	-	-	861	830	3	10	γ CC(12) + β CCC(39)
37	851(w)	848(vw)	852	821	30	1	t HCCC (35)+out of CCCC(11)
36	-	-	830	800	3	0	t HCCC(77)
35	-	-	825	796	7	0	t HCCC(62)
34	782(ms)	-	819	789	10	62	γ OC (18) + β CCC(24)
33	-	769(vw)	771	743	14	4	t HCCC(18) + t CCCC(10) + out of torsion OCCC(17)
32	717(s)	723(w)	751	724	57	0	t HCCC(69) + out of torsion OCCC(17)
31	-	-	734	708	17	1	v CC(10) + β CCC(18)
30	-	-	721	695	2	0	t CCCC(51)
29	669(w)	687(w)	680	656	28	35	v BrC(11) + β CCC(13)
28	-	-	671	647	2	0	t CCCC (23) + out of torsion CCCC(25)
27	647(w)	658(w)	650	627	15	5	β OCC(18) + β CCC(25)
26	-	633(w)	638	615	19	5	β CCC(37) + β OCC(15)
25	-	573(w)	578	557	3	27	β OCC(34) + β CCC(11) + β COC(17)
24	550(ms)	-	565	545	3	13	β CCC(40)
23	543(ms)	-	531	512	2	0	t HCCC(29) + t CCCC(13) + out of OCCC(34)
22	-	-	497	479	23	0	t HCCC(10) + t CCCC(16) + out tor BrCCC(15) + out CCCC(22)
21	438(w)	-	444	428	1	3	β CCC(17) + β COC(17)
20	-	-	431	415	0	0	t CCCC(55)
19	404(w)	-	413	398	0	0	t HCCC(12) + t CCCC(64)
18	-	385(vw)	387	373	7	1	v CC(10) + β CCC(33)
17	-	-	381	367	5	3	v CC (22) + β OCC(23)
16	-	-	319	308	2	1	v Br C(29) + β COC (15)
15	-	310(vw)	313	302	0	1	out of torsion BrCCC(36) + out CCCC(4)

							+ t CCCC(12)
14	-	-	282	272	0	1	t HOCC(25) + t HCOC (20)
13	-	-	275	265	5	1	β OCC(29) + β COC (30)
12	-		233	224	0	1	t CCCC(40) + t COCC(10)+ t OCCC(13)
11	-	211(w)	232	224	1	1	β CCC(11) + β BrCC(49)
10	-	155(w)	159	154	2	0	β CCC(36)
9	-	138(w)	138	133	1	2	t CCCC(56) + out of tor BrCCC(22)
8	-	119(vw)	132	127	1	1	v CC(10) + β CCC(24)
7	-	105(w)	101	98	0	3	t CCCC(45) + t HOCC(12)
6	-	88(w)	97	94	3	1	t HCOC(10)+ t CCCC(10)+ t COCC(60)
5	-	65(w)	51	49	1	1	β CCC(52) + v CC(29)
4	-	-	36	35	0	0	t CCCC(55) + out of tor CCCC(19)
3	-	-	22	22	0	1	t CCCC(89)
2	-	-	16	16	3	1	t CCCC(79)
1	-	-	10	10	0	1	t HCCC(10) + t CCCC(47)

Note : s: strong, vs: very strong, m: medium, ms: medium strong, w: weak, v:stretching,β: in plane bending, γ: out of plane bending, t: torsion, sym: symmetric stretching,asym: asymmetric stretching,

a Scaling factor: 0.961 for DFT(B3LYP)/6-311++G(d,p).
b Relative absorption intensities normalized with highest peak absorption equal to 100.
c Relative Raman intensities normalized to 100.

Table 3.The electric dipole moments (Debye), polarizability (in esu), β components and β_{tot} (10^{-30}esu) value of title compound calculated by B3LYP/ 6-311++G(d,p) method

.

Parameter	B3LYP/6-311++G(d,p)	Parameter	B3LYP/6-311++G(d,p)
μ_x	1.092362	βxxx	1101.8834
μ_y	-0.930407	βxxy	1174.2724
μ_z	-0.0000397	βxyy	767.9546
μ(D)	1.4348	βyyy	211.45786
α_{xx}	340.4961	βzxx	-0.22492
α_{xy}	80.909	βxyz	0.05998
α_{yy}	263.5495	βzyy	0.2361
α_{xz}	0.00022	βxzz	40.9022
α_{yz}	-0.00057	βyzz	-74.8852

α_{zz}	108.7203	βzzz	-0.1822
a (e.s.u)	$1.611x\ 10^{-23}$	βtot (e.s.u)	$1.574x10^{-23}$
Δa (e.s.u)	$2.3879x10^{-48}$		

Table 4.Second order perturbation theory analysis of Fock matrix in NBO basis.

Donor	**Type**	**ED/e**	**Acceptor**	**Type**	**ED/e**	**E(2)**	**E(j) -E(i)**	**F(i,j)**
C_1 - C_2	σ	1.97431	C_1 - O_4	σ*	1.98743	3.77	1.38	0.064
			C_2 - C_3	σ*	1.9734	3.61	1.38	0.063
			C_3 - C_{13}	σ*	1.95997	2.96	1.37	0.057
C_1 - O_4	σ	1.98743	C_1 - C_2	σ*	1.97431	3.72	1.67	0.071
			C_2 - C_3	σ*	1.9734	1.1	1.7	0.039
			C_5 - C_{10}	σ*	1.95942	1.66	1.7	0.048
	π	1.92106	C_2 - C_3	π*	1.80093	10.36	0.39	0.058
			C_5 - C_6	π*	1.59105	7.12	0.4	0.053
C_1 - C_5	σ	1.95997	C_1 - C_2	σ*	1.97431	5.49	1.34	0.077
			C_1 - O_4	σ*	1.98743	3.76	1.37	0.064
			C_2 - H_{20}	σ*	1.96957	2.67	1.13	0.049
C_2 - C_3	σ	1.9734	C_1 - C_2	σ*	1.97431	3.07	1.36	0.058
			C_1 - O_4	σ*	1.98743	3.91	1.39	0.066
			C_2 - H_{20}	σ*	1.96957	1.13	1.15	0.032
	π	1.80093	C_1 - O_4	π*	1.92106	29.35	0.32	0.088
			C_9 - C_{10}	π*	1.97004	1.37	0.32	0.019
			C_{13} - C_{14}	π*	1.60785	19.73	0.32	0.075
C_2 - H_{20}	σ	1.96957	C_1 - C_2	σ*	1.97431	1.17	1.15	0.033
			C_1 - O_4	σ*	1.98743	0.98	1.17	0.03
C_3 - H_{21}	σ	1.7786	C_1 - C_2	σ*	1.97431	0.56	1.05	0.023
			C_2 - H_{20}	σ*	1.96957	4.37	0.85	0.057
			C_3 - H_{21}	σ*	1.7786	22.95	1.31	0.155
			C_9 - C_{10}	σ*	1.97004	3.8	1.08	0.06
			C_{10} - H_{25}	σ*	1.77473	200.28	1.31	0.461
C_5 - C_6	σ	1.95613	C_1 - C_2	σ*	1.97431	2.44	1.36	0.051
			C_1 - C_5	σ*	1.95997	7.15	1.35	0.088
			C_5 - C_{10}	σ*	1.95942	7.74	1.39	0.093

			C_6 - C_7	σ*	1.9704	6.97	1.38	0.088
	π	1.59105	C_1 - O_4	π*	1.92106	27.78	0.31	0.087
			C_5 - C_6	π*	1.59105	1.7	0.32	0.021
			C_7 - C_8	π*	1.68114	18.45	0.31	0.069
			C_9 - C_{10}	π*	1.97004	24.37	0.31	0.079
C_7 - C_8	σ	1.97033	C_6 - C_7	σ*	1.9704	4.9	1.38	0.073
			C_6 - O_{11}	σ*	1.98823	4.41	1.12	0.063
			C_7 - H_{22}	σ*	1.97071	1.94	1.14	0.042
			C_8 - C_9	σ*	1.97111	4.45	1.38	0.07
			C_8 - H_{23}	σ*	1.97882	1.3	1.15	0.035
			C_9 - H_{24}	σ*	1.97648	3.3	1.15	0.055
	π	1.68114	C_5 - C_6	π*	1.59105	25.36	0.32	0.082
			C_9 - C_{10}	π*	1.68065	19.38	0.31	0.07
C_7 - H_{22}	σ	1.97071	C_5 - C_6	σ*	1.95613	3.94	1.15	0.06
			C_6 - C_7	σ*	1.9704	1.52	1.16	0.038
C_9 - C_{10}	σ	1.97004	C_9 - H_{24}	σ*	1.97648	1.43	1.14	0.053
			C_{10} - H_{25}	σ*	1.77473	1.61	1.61	0.047
			C_5 - C_6	π*	1.59105	19.63	0.31	0.072
			C_7 - C_8	π*	1.97033	24.4	0.31	0.078
			C_5 - C_{10}	σ*	1.95942	4.15	1.16	0.062
	π	1.68065	C_8 - H_{23}	σ*	1.97882	0.69	0.92	0.023
			C_9 - C_{10}	σ*	1.97004	1.4	1.16	0.036
C_9 - H_{24}	σ	1.97648	C_{10} - H_{25}	σ*	1.77473	1.17	1.39	0.038
			C_1 - C_5	σ*	1.95997	0.53	1.04	0.022
			C_3 - C_{13}	σ*	1.95997	3.99	1.06	0.061
			C_3 - H_{21}	σ*	1.7786	206.57	1.3	0.465
C_{13} - C_{14}	σ	1.95716	C_{15}- H_{30}	σ*	1.97405	2.89	1.12	0.051
			C_{18} - H_{32}	σ*	1.97094	2.83	1.14	0.051
			C_2 - C_3	π*	1.80093	21.93	0.31	0.079
			C_{15} - C_{16}	π*	1.67329	24.95	0.29	0.077
			C_{17} - C_{18}	π*	1.96266	20.46	0.31	0.073
C_{15} - C_{16}	σ	1.97374	C_{13} - C_{14}	π*	1.60785	18.62	0.33	0.071
			C_{13} - C_{18}	π*	1.95302	20.8	0.33	0.075

			C_{13} - C_{14}	σ*	1.95716	3.43	1.13	0.056
C_{17} - C_{18}	σ	1.96266	C_{18} - H_{32}	σ*	1.97094	1.52	1.15	0.038
			C_{13} - C_{14}	π*	1.60785	22.47	0.32	0.077
			C_{15} - C_{16}	π*	1.67329	22.21	0.3	0.073
			C_{13} - C_{18}	σ*	1.95302	3.52	1.13	0.057
C_{18} - H_{32}	σ	1.97094	C_{17} - H_{31}	σ*	1.9747	0.71	0.92	0.023
			C_1 - C_2	σ*	1.97431	1.58	1.29	0.041
			C_1 - C_5	σ*	1.95997	1.15	1.28	0.035
			C_5 - C_6	σ*	1.95613	1.02	1.15	0.031
LP(1) O_4	σ	1.98125	C_{12} - H_{27}	σ*	1.993	0.85	0.87	0.024
			C_{12} - H_{28}	σ*	1.993	0.86	0.87	0.025
LP(1) O_{11}	σ	1.9607	C_5 - C_6	π*	1.59105	30.74	0.35	0.099
			C_{15} - C_{16}	σ*	1.97374	1.73	1.63	0.048

E(2)[a] means energy of hyper conjugative interaction (stabilization energy).
E(j)–E(i)[b] Energy difference between donor and acceptor i and j NBO orbitals.
F(i, j)[c] is the Fock matrix element between i and j NBO orbitals.

Table 5: Hydrogen bonding and molecular docking with antimicrobial protein targets

Protein (PDB ID)	Bonded residues	No. of hydrogen bond	Bond distance (Å)	Estimated Inhibition Constant (μm)	Binding energy (kcal/mol)	Reference RMSD (Å)
4Y95	TRP 395	3	3.6	7.04	-7.03	36.958
	ILE 347		4.7			
	TRP 421		4			
ZH4Z	TRP 85	3	1.7	32.29	-6.13	92.28
	VAL 59		3.3			
	CYS 145		3.7			